

Cortical Imaging Through the Intact Mouse Skull Using Two-Photon Excitation Laser Scanning Microscopy

ELIZABETH J. YODER* AND DAVID KLEINFELD

Department of Physics, University of California, San Diego, La Jolla, California 92093-0319

Two-photon excitation scanning microscopy has several advantages for imaging brain cells and other anatomical features in whole animals (Denk et al., 1994). These advantages stem from three main factors. The first is the quadratic dependence of optical absorption, so that optical sectioning is performed solely by the incident light. The second is the use of infrared light, which scatters less than visible light and hence increases the depth of focal penetration. The third is the use of a point-scanning system to optimize spatial resolution. The application of two-photon microscopy for in vivo imaging has typically utilized a surgically-prepared “cortical window” in which a section of the skull has been replaced by a agarose plug that is sealed with a glass coverslip (Svoboda et al., 1997). While this method adequately controls for motion due to cardiac and respiratory rhythms, the “cortical window” preparation renders the brain susceptible to fluctuations in temperature and pressure. In contrast, intrinsic optical imaging techniques are performed through thinned, intact skull, thus protecting the brain from external influences (Masino et al., 1993). However, the spatial resolution of intrinsic optical imaging is insufficient to visualize fine features like single cells or capillaries. In an effort to image the brain with subcellular spatial resolution and without the “cortical window” procedure, a method was devised to image directly through thinned mouse skull using two-photon excitation microscopy.

The use of mice for these studies was motivated on two fronts. First of all, the murine *dura mater* is of negligible thickness and does not impede cellular imaging deep in the brain. Secondly, since mouse cortex is only 70–75% as thick as rat cortex, more cortical anatomy may be imaged for a given depth of penetration. This is a salient point, as the attainable cortical penetration is reduced by the depth of the thinned skull. NIH Swiss mice ($n = 12$) were anesthetized with urethane (1.5 g/kg i.p.) and placed into a small animal stereotaxic apparatus (Slotnick, 1972) with a mouse adaptor (Kopf 926) and custom-built head supports. Body temperature was maintained by a heating blanket that was regulated via feedback from a rectal thermoprobe. The skin over the skull was reflected and the imaging region was marked. The skull was dried and the imaging region was thinned to $\sim 250 \mu\text{m}$ using a high-speed air drill and FG1/2 or FG3/4 burr. No bone wax was applied. The rest of the skull was covered with thin superglue (Loctite 293). A stainless steel headframe, modified from an earlier design (Kleinfeld and Denk, 2000), was sealed to the skull with dental cement (Fig. 1). The headframe was secured to the imaging apparatus. Artificial cerebral spinal fluid (ACSF) was applied over the imaging region and images were

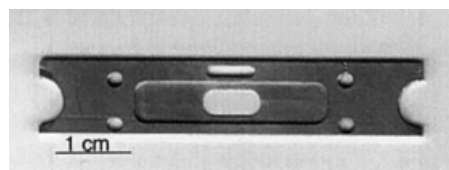


Fig. 1. Design of the headframe used to image through intact mouse skull. The center ellipse is placed over the region to be imaged. The surrounding recessed area serves as a reservoir for ACSF, so that the skull may be kept moist. This headframe may also be used for imaging through a cortical window.

obtained using a water immersion objective lens (Zeiss $40\times$ NA = 0.8 or $63\times$ NA = 0.9) that was placed directly in the ACSF over the skull.

Angiography of the cerebral vasculature was accomplished via a bolus injection into the mouse tail vein of $50 \mu\text{l}$ of a fluorescent solution (5% FITC-dextran, MW 75K). Two-photon excitation was accomplished with the use of a commercial mode-locked Titanium-Sapphire laser system (Coherent Verdi-Mira, 100 fsec pulse width pumped at 10 W, repetition rate of 76 MHz) that was tuned to 800 nm. The maximum average power exiting the objective lens was 180 mW for $40\times$ (NA = 0.8) and 200 mW for $63\times$ (NA = 0.9). The cortical surface was imaged at low power (15 mW for $40\times$) and the power was incrementally increased for deeper imaging up to a maximum penetration of $500 \mu\text{m}$ (half of which was through the skull). Fluorescent emission was recorded by an external photomultiplier tube after passing through laser blocking filters (BG39 and BG40) and a fluorescein emission filter (525–535 nm). Sample data are shown in Figures 2 and 3.

In general, “through-skull” imaging procedures enabled longer recording periods than were observed with “cortical window” preparations. This effect may be attributed to the protection of the brain from external changes in temperature and pressure by the thinned skull. While the procedures that have been described were used to visualize the cerebral vasculature of NIH Swiss mice, these methods are applicable to any preparation that involves imaging fluorescence in mouse brain (Yoder, 2002). Examples of other applications include visualizing intracellularly injected fluorescence

*Correspondence to: Dr. Elizabeth Yoder, Dept. of Radiology, UCSD Medical Center, 410 Dickinson Street, San Diego, CA 92103-8749.
E-mail: eyoder@ucsd.edu

Contract grant sponsor: NIH; Contract grant numbers: MH12420, RR13419, NS041096; Contract grant sponsor: Packard Foundation.

Received 10 May 2001; accepted in revised form 27 July 2001

Fig. 2. Cerebral vascular angiogram as visualized through the intact, thinned skull. This image was obtained by Kalman averaging ($n = 8$). The focal plane is located 105μ beneath the base of the skull. The line through a capillary segment was repeatedly scanned in time at a rate of 500 Hz with an average power of 90 mW exiting the objective lens. (Data is presented in Fig. 3.)

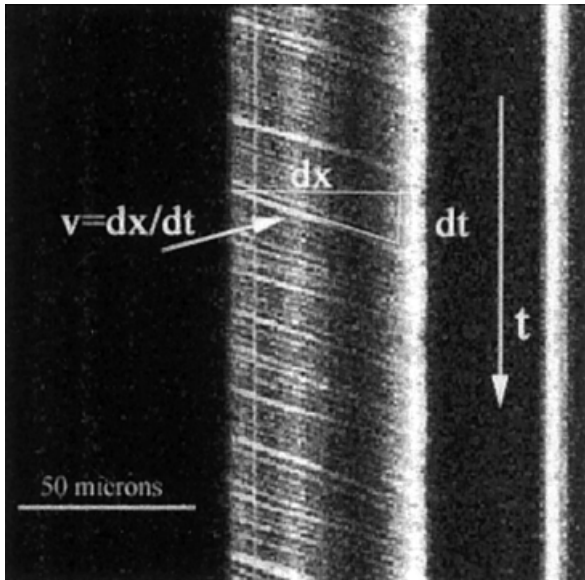
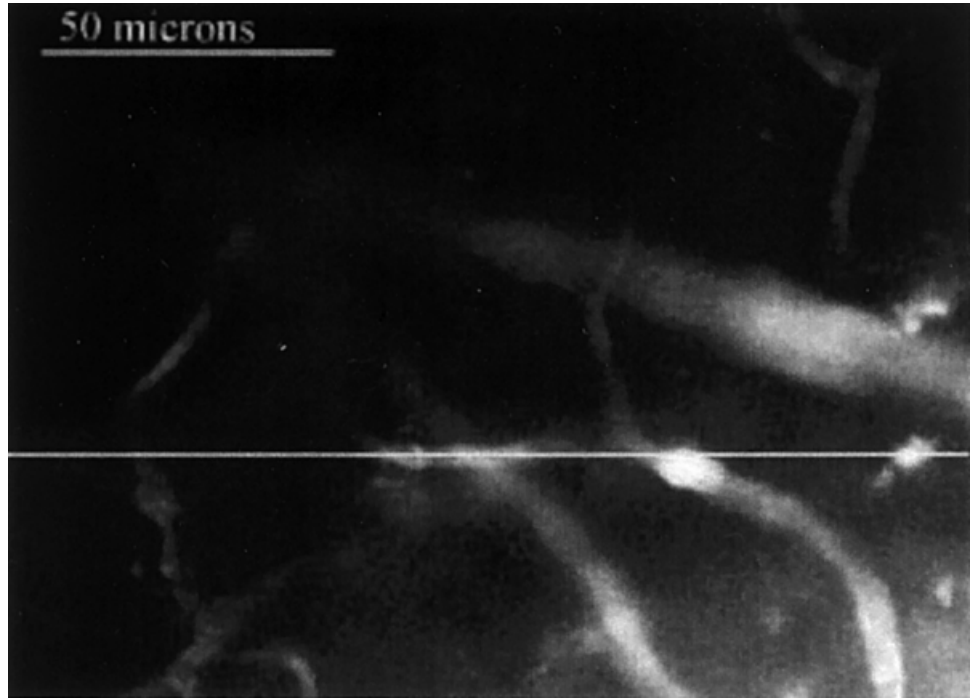


Fig. 3. Red blood cell motion within the capillary segment indicated in Figure 2, as detected through intact skull via line scan (XT) acquisition mode. The unlabeled cells appear as dark bands that are contrasted against the fluorescent blood serum. Red blood cell velocity, v , is determined by the slope of its band, as indicated. This data was collected using a $40\times$ water immersion lens ($NA = 0.8$).

or imaging transgenic mice that express genetically encoded fluorescence (e.g., green fluorescent protein).

REFERENCES

- Denk W, Delaney KR, Gelperin A, Kleinfeld D, Strowbridge BW, Tank DW, Yuste R. 1994. Anatomical and functional imaging of neurons using 2-photon laser scanning microscopy. *J Neurosci Methods* 54:151–162.
- Kleinfeld D, Denk W. 2000. Two-photon imaging of neocortical microcirculation. In: Yuste R, Lanni F, Konnerth A, editors. *Imaging neurons*. Cold Spring Harbor, NY: Cold Spring Harbor Laboratory Press. p 23.1–23.15.
- Masino SA, Kwon MC, Dory Y, Frostig RD. 1993. Characterization of functional organization within rat barrel cortex using intrinsic signal optical imaging through a thinned skull. *Proc Natl Acad Sci USA* 90:9998–10002.
- Slotnick BM. 1972. Stereotaxic surgical techniques for the mouse. *Physiol Behav* 8:139–142.
- Svoboda K, Denk W, Kleinfeld D, Tank D. 1997. In vivo dendritic calcium dynamics in neocortical pyramidal neurons. *Nature* 385: 161–165.
- Yoder EJ. 2002. In vivo microscopy of the mouse brain using multiphoton laser scanning techniques. *SPIE Proceedings* 4620: in press.